*Central European Journal of Energetic Materials*, **2012**, *9*(1), 17-38
ISSN 1733-7178

# Numerical Analysis of the Deflagration to Detonation Transition in Primary Explosives

Waldemar A. TRZCIŃSKI

*Military University of Technology,*
*Faculty of Advanced Technology and Chemistry*
*Kaliskiego 2, 00-908 Warsaw, Poland*
*E-mail: wtrzcinski@wat.edu.pl*

**Abstract:** Theoretical models proposed in the literature for the deflagration-to-detonation transition (DDT) in cast explosives are evaluated for primary explosives (complex compounds) in this work. The one-dimensional model of burning (deflagration), consistent with the classical Chapman-Jouguet theory and a model of burning under the conditions of zero mass velocity behind the flame front are presented, and the physical phenomena accompanying the accelerating wave of flame in solid explosives are described. The results of calculations taken from the literature are presented for the cast high explosive (pentolite). The model of acceleration of the deflagration wave was used to estimate the time and distance at which the process of burning leads to the emergence of a shock wave in primary explosives. The influence of burning rate and the physical properties of an explosive on the distance of deflagration to detonation transition is analysed.

**Keywords:** explosives, deflagration to detonation transition

## Introduction

From the huge number of experimental studies of the process of deflagration to detonation transition (DDT) in the detonation of condensed explosives, the following conclusions can be drawn [1]:

- the most important difference between the DDT process in primary and secondary explosives is the speed of transition from deflagration to detonation − in the case of primaries the process is much faster;
- because the difference is rather quantitative than qualitative, all the

relationships derived for secondaries can also be applied to primaries;
- it is far easier to build a quantitative model for the DDT process in cast explosives than in porous materials.

The first conclusion comes from the prime function of primary and secondary explosives. Since primaries need to have undergone a violent detonation, if only by being exposed to the heat pulse, whilst the detonation of secondary explosives is mainly initiated by the shock wave. It is commonly believed that the faster the DDT, the better the primary material is. The ease of the transition to detonation is also a weakness of primary explosives, because accidental ignition leads to detonation.

The second conclusion results from the observation of many similarities between primary and secondary explosives in the DDT process. Both types of materials are subject to this process, but in the case of secondary explosives the transition takes longer and the charge needs to be enclosed in heavy confinement.

The final conclusion follows from the results of the DDT process in cast explosives and good agreement between the experimentally determined time and distance of detonation development with data received from the one-dimensional model of Macek [2]. There is no similar model for the transition to detonation in the case of porous explosives. The experimental data confirm the existence of a convective flame front with high surface area in these materials and, consequently, the formation of a complex flow field, affecting the DDT process. Over the years, a consensus has been reached on the mechanism controlling the DDT process [3-6]. Convective flow and hot-gas ignition contribute only initial, low velocity phenomena. The formation of a compaction wave in undisturbed material begins a series of non-convective events that lead to the final shock-to-detonation (type I DDT). Another mechanism was observed for low density charges. In this case, the outbreak of detonation is preceded by a rapid build-up of pressure at the point where the detonation occurs (type II DDT) [7-9].

There are complex numerical models in which the porous explosive is treated as a two-phase mixture of interacting continua, consisting of grains of reacting solid and the gaseous products of combustion [10-12]. At the moment, there is no simple physical model taking into account the complexity of the DDT in porous explosives.

In this paper, the one-dimensional model proposed in [2] and developed in [1] is used to predict the path of transition of burning to detonation in primary explosives. In the first part, Macek's model of the development of deflagration to detonation in cast secondary explosives is described. A critical analysis of this model given in work [1] is also presented. This is followed by a description of the one-dimensional model of burning (deflagration), consistent with the classical

CJ theory, and the physical phenomena accompanying the accelerating wave of flame in solid explosives is discussed. Details of models of the DDT analyzed in [1] and the results of the calculations presented are considered. Finally, the acceleration model is used to estimate the time and distance at which the process of burning leads to the emergence of a detonation wave in primary explosives. The influence of the burning rate and the physical properties of the explosive on the distance of the DDT is analyzed.

## Macek's model for DDT

If the deflagration wave is initiated at the bottom of a closed tube, it propagates into the explosive and generates a stream of gas in the opposite direction to the wave motion. Since these gases stop at the bottom of the tube, their kinetic energy changes in internal energy. Increasing pressure in the gas is the source of compression waves which interact with the wave and accelerate the movement of the deflagration flame (Figure 1). Moving faster and faster, the combustion front generates in turn compression waves in the unreacted explosive before the flame front, which creates a complex, unsteady flow. The interaction of compression waves creates a shock wave inside the material. This wave initiates reactions leading to generation of a detonation wave. The amplitude of the shock wave which initiates detonation depends on the type of explosive.

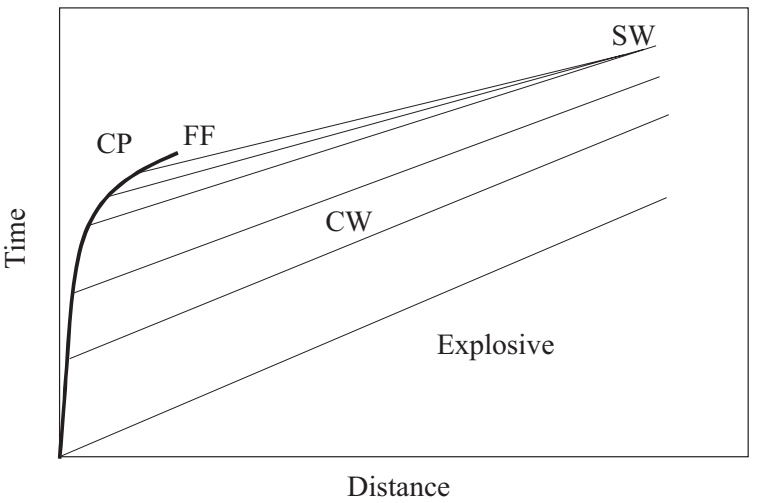


**Figure 1.** DDT in a distance-time diagram: CP − combustion products, FF − flame front, CW − compression waves, SW − shock wave.

The mechanism of increase in pressure in the flame front depends on the type of fuel. Turbulence and possible diffusion of hot combustion products are the dominant phenomena in gases and porous solid explosives. In homogeneous explosives, these processes are absent, and the main mechanism of increase in pressure is accelerated by laminar burning [13].

The conditions necessary for the formation of a shock front in a burning explosive are strictly defined [2]. Firstly, it is necessary to limit the flow of the resulting combustion products to the rear. This provides increased pressure acting on the explosive and generates in it disturbances in the direction of propagation of the flame wave. The leading edge of these disturbances, according to "the accelerating piston mechanism", transforms into a shock front. If expansion of combustion products is unrestricted, the pressure does not rise sufficiently to form a shock wave in the explosive. Secondly, the increase in pressure must be rapid. Since the compression waves are catching up and generate a shock wave inside the charge, the time needed to increase pressure from the baseline value to the value on the initiating shock wave must be lower than the time of passage of the sound wave by the charge.

Macek [2] proposed the first generation of experimental and theoretical methods for testing the DDT phenomenon in secondary explosives. He measured the time-dependence of the pressure in the combustion products of the explosive enclosed in a metal tube, and the time and place of the emergence of the detonation wave in the explosive. The dependence of the measured pressure $p$ in the combustion products on the time $t$ was approximated by the function:

$$p = p_0 e^{at} \tag{1}$$

where $p_0$ is the initial pressure and $a$ is an experimentally determined constant. Macek assumed that the pressure in the combustion products is equal to the pressure in the explosive. Macek described continuous compression of the explosive by the modified Tait equation:

$$p = \frac{\rho_0 c_0^2}{n}\left[\left(\frac{\rho}{\rho_0}\right)^n - 1\right] \tag{2}$$

where $\rho$, $\rho_0$ and $c_0$ are mean density, initial density and velocity of sound in the explosive, and $n$ is a constant.

The movement of the compression waves in the explosive was calculated in [2] by the method of characteristics. Macek assumed that $n = 3$, so that the

characteristics C+ in the compression wave are straight lines (Figure 1). The point of intersection of the characteristics on which the difference in pressure is a few kbar, was assumed as the beginning of the formation of the shock wave of such an amplitude as to be able to boost the explosive to detonate. The initiated detonation wave travels through the material in the direction of propagation of the flame front (detonation) and in the opposite direction (retonation).

Using such an approximation, Macek obtained good agreement between the calculated times and distances to detonation transition and measured values (time ~ 100 μs, distance ~12 cm) for the two high explosives − diethylnitramine dinitrate (DINA) and pentolite (PETN/TNT 50/50) [2]. Macek also attempted to clarify the apparent exponential relationship between pressure and time behind the front, using a one-dimensional adiabatic model of burning. The dependence of the linear flame front speed $U$ on the pressure $p$ had the form:

$$U = \beta p^{\lambda} \tag{3}$$

where $\beta$ and $\lambda$ are constants. The author of work [2] assumed that for the tested materials $\lambda = 1$ and $\beta = 10$ cm/sec kbar. The resulting time-dependence of the pressure matched equation (1) by a constant of proportionality, which takes into account the size of the flame front surface.

Although Macek obtained quantitatively good agreement between the experimental data and the calculated results for two high explosives, according to the authors of work [1] the theoretical model has weaknesses. Firstly, assuming that the pressures in the combustion products and the explosive are equal, Macek ignored the pressure drop at the deflagration wave front, which can be significant if the process reaches the deflagration CJ regime. According to the CJ theory, the pressure in unreacted material can be much higher than the pressure in combustion products. Secondly, the dependence of the linear burning velocity on pressure describes well the experimental dependence for only about 1 kbar pressure. The actual relation between the burning rate and pressure in the process of an accelerating deflagration wave, which generates a detonation wave, is different from the burning rate law (3). The third weak point of Macek's analysis is the omission of momentum transferred to the reaction products at the deflagration wave front. In the case of a closed tube, the energy associated with the movement of particles in fact affects the acceleration of the flame front.

## Models of DDT taking into account the properties of the deflagration wave

Figures 2 and 3 show, on the pressure-volume and pressure-particle velocity planes, schematic Hugoniot curves for the reaction products of an explosive in the case of detonation and deflagration [1]. The upper curves and the CJ points correspond to detonation, while the lower curves and CJ' points are related to the deflagration. The parameters of the CJ' point correspond to a stationary combustion wave propagating in an explosive.

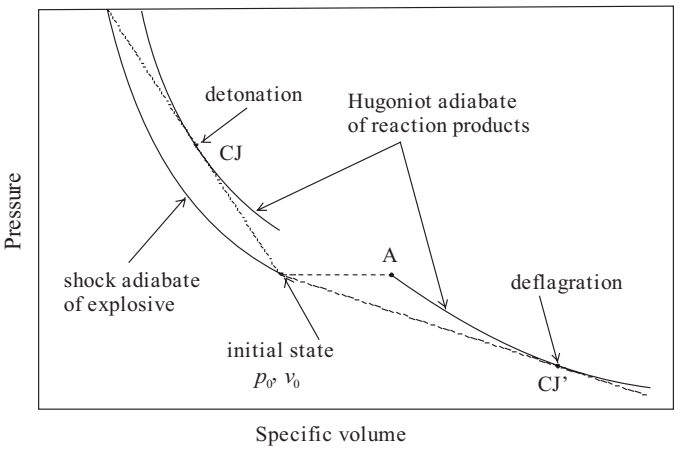


**Figure 2.** Pressure-volume diagram for deflagration and detonation [1].

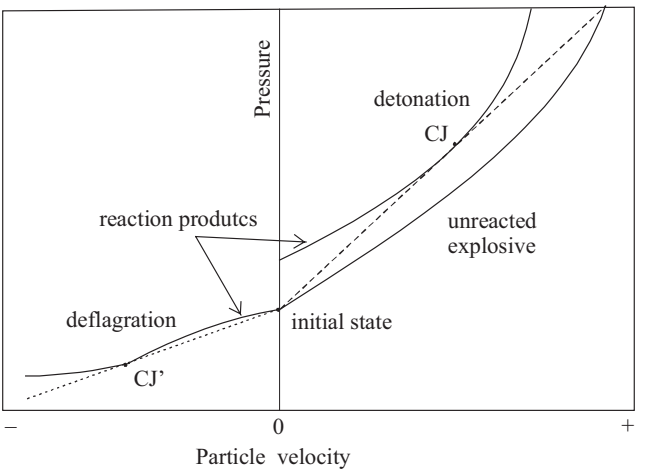


**Figure 3.** Pressure-particle velocity diagram for deflagration and detonation [1].

As previously stated, a deflagration wave initiated at the bottom of a closed tube moves along the tube and burns the explosive, generating the reaction products moving in the opposite direction. The reaction products are decelerated at the bottom of the tube and their kinetic energy transforms into internal energy. As a result, the pressure increases and compression waves propagate in the products, causing acceleration of the deflagration wave. The accelerating flame front, in turn, generates a compression wave in the explosive which leads to a complex unsteady flow ahead of the front. The initial state of the unreacted explosive is the compressed state.

This complex movement associated with the accelerating deflagration wave is illustrated in Figure 4 using particle velocity-distance diagrams [1]. For simplicity, the deflagration wave front was presented as a discontinuity, although in reality it has a finite width. In Figures 4a and 4b, the mass velocity of the reaction products on the front of the deflagration wave is negative and the occurrence of a compression area is necessary to reach a value of zero at the bottom of the tube. Figure 4c shows a case in which the mass velocity drop at the deflagration wave front is exactly equal to the mass velocity of the compressed material before the front. In the next phase of acceleration of the deflagration wave (Figure 4d) mass velocity behind the wave front is positive and it is necessary to create an expansion area to satisfy the boundary condition at the bottom of the tube. However, when the compression zone behind the wave front no longer exists, then the mechanism of acceleration of the deflagration wave associated with the process of gas compression also vanishes.

Although the exact solution of the complex unsteady flow generated by the deflagration wave in a closed tube is very difficult, there are two analytical models of the process of combustion wave acceleration which allow the upper and lower limits of combustion velocity to be estimated in a relatively simple way. For the detonation wave only the CJ point corresponds to a stable process, but in the case of the deflagration wave, the final state of the products can be identified by any point on the Hugoniot curve between points A and CJ'(Figures 2 and 3), namely the so-called weak deflagration branch. Point A corresponds to a hypothetical deflagration at constant pressure, during which the mass velocity does not change, but the CJ' point is associated with deflagration, for which the combustion wave velocity, mass velocity and pressure reduction are the largest.

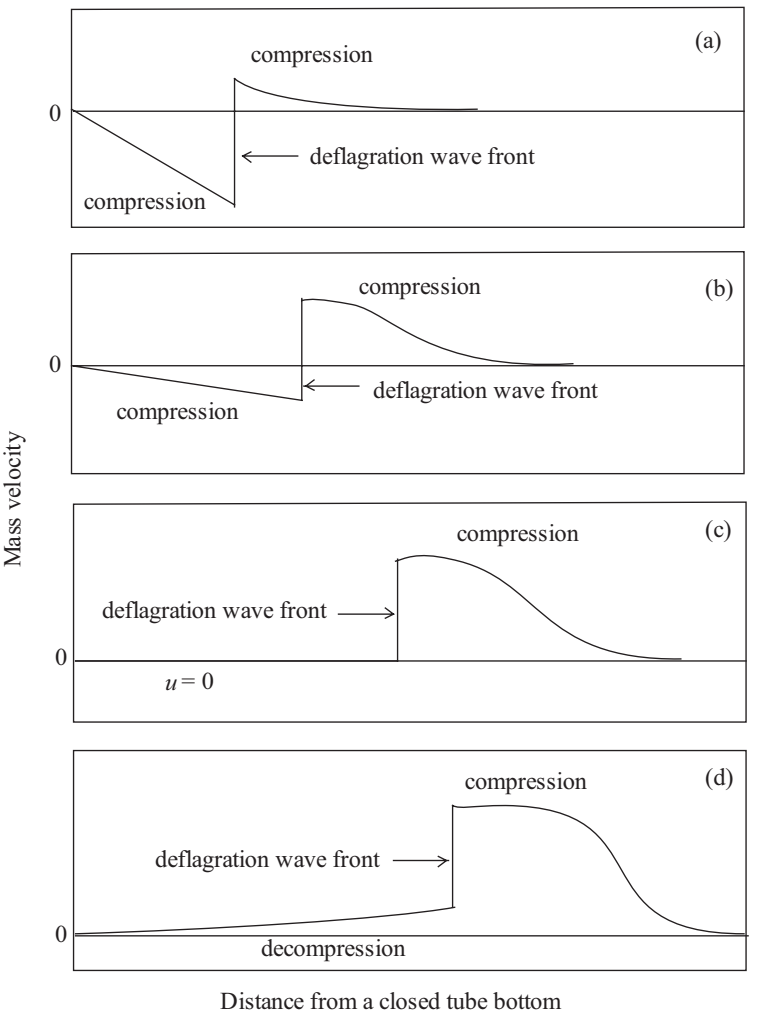


**Figure 4.** Particle velocity-distance diagrams for accelerating deflagration waves [1].

Taking into account the above-described mechanism of acceleration and deflagration wave properties, the authors of work [1] have considered two analytical models describing the process of flame acceleration. In the first, proposed by Adams and Pack [14] to describe deflagration waves in gases, there is a compression area of the explosive terminated by the deflagration wave whose velocity is such that the momentum of compressed explosive is exactly equal to the momentum fall at the wave front and the mass velocity of reaction products

is zero (Figure 4c). In this model, there must be no rarefaction or compression waves in the reaction products to meet the boundary condition at the bottom of the tube. Since the change in particle velocity with distance behind the front of the combustion wave is zero, the pressure change in the time on the left border must also be zero. Although in this model the law of conservation of momentum is fulfilled, it is not physically correct because it is not possible in this model to accelerate the flame and there is no mechanism to increase pressure at the bottom of the tube. However, the model of Adams and Pack allows the lower flame velocity and the pressure drop at the front of the accelerating deflagration wave to be designated, since for each wave propagating with a faster speed there is a decrease in mass velocity at its front and it is possible to realize a mechanism of flame acceleration.

In the second model it is assumed that deflagration is always the CJ wave with the greatest possible velocity of propagation and with the biggest drop in pressure at the front. This model allows the mechanism of flame acceleration in accordance with the scheme shown in Figure 4 to be described. It was used for the first time by Troshin to study the DDT process in gases [15]. An interesting state of deflagration, where the two models provide the same mass velocity and pressure in the reaction products, is the case shown in Figure 4c. For the CJ deflagration, this state corresponds to the case when the stage of flame acceleration and generation of new compression waves ends. Table 1 shows, as calculated in [1], the parameters of this state for TNT and pentolite. The values obtained for the compression wave, 95 kbar for TNT and 129.5 kbar for pentolite, are too big to be a criterion for DDT, because for pentolite its sensitivity to the shock wave is about 20 kbar, and cast TNT can be initiated by a shock wave with an amplitude of 60 kbar. The transition from burning to detonation in pentolite is relatively easy, in TNT it is impossible. Thus, there is another criterion of flame acceleration which determines whether the transition from deflagration to detonation occurs in a cast explosive.

**Table 1.** CJ deflagration wave parameters of zero-mass velocity behind the wave front [1]

| Deflagration wave parameters | Cast TNT | Pentolite |
|---|---|---|
| Shock pressure in explosive [kbar] | 95.0 | 129.5 |
| CJ deflagration velocity [mm/μs] | 3.116 | 3.504 |
| CJ pressure after deflagration [kbar] | 43.5 | 63.4 |

In the paper [1] the discussed models of acceleration of flame were used to calculate the transition from burning to detonation in pentolite. To determine

the time and distance of creation of a shock wave in the explosive ahead of the flame front, the method of characteristics was used. The time-dependence of pressure in the combustion products of pentolite for the pressure below 1 kbar was described by Macek's relationship [1] with the parameters $p_0 = 0.08$ kbar, $a = 0.12$ 1/μs, and for the pressure above 1 kbar by the relation given in [16]:

$$p_2 = (1\text{kbar})e^{0.8856(t\text{-}21.05)} \tag{4}$$

where $p_2$ is the pressure behind the front of the deflagration wave. Time $t$ is expressed in microseconds.

To describe the physical properties of the explosive, the modified Tait equation (2) with $n = 3$ was applied for isentropic compression. Using the relations valid along the set of negative characteristics $C_-$, the speed of sound $c_1$, mass velocity $u_1$, density $\rho_1$ and the internal energy $e_1$ of the compressed explosive in front of the deflagration wave were determined along the straight positive characteristics $C_+$ as a function of the pressure $p_1$:

$$\rho_1 = \rho_0 \left( 1 + \frac{3\,p_1}{\rho_0\, c_0^2} \right)^{1/3} \tag{5}$$

$$u_1 = c_0 \left[ \left( 1 + \frac{3\,p_1}{\rho_0\, c_0^2} \right)^{1/3} - 1 \right] \tag{6}$$

$$u_1 + c_1 = c_0 \left[ 2\left( 1 + \frac{3\,p_1}{\rho_0\, c_0^2} \right)^{1/3} - 1 \right] \tag{7}$$

$$e_1 - e_0 = \frac{p_1}{2\rho_1} - \frac{c_0^2}{2}\left( 1 - \frac{\rho_0}{\rho_1} \right) \tag{8}$$

where $\rho_0$, $c_0$ are the parameters of equation (2), $e_0 = c_0^2/2$.

The laws of conservation of mass, momentum and energy flow at the deflagration wave front can be written in the following form:

$$\rho_1(w - u_1) = \rho_2(w - u_2) \tag{9}$$

$$p_1 + \rho_1(w - u_1)^2 = p_2 + \rho_2(w - u_2)^2 \tag{10}$$

$$e_1 + \frac{p_1}{\rho_1} + \frac{(w-u_1)^2}{2} + q = e_2 + \frac{p_2}{\rho_2} + \frac{(w-u_2)^2}{2} \tag{11}$$

where the index 2 refers to the parameters behind the deflagration front, $w$ denotes the velocity of the deflagration wave and $q$ is the heat of reaction.

The physical properties of the gaseous reaction products are described by a polytropic gas model, for which the relations are true:

$$\frac{p_2}{\rho_2^k} = \text{const} \tag{12}$$

$$p_{CJ} = \frac{\rho_0 D^2}{k+1} \tag{13}$$

where $k$ is the adiabatic exponent of the reaction products. In the paper [1] its value was proposed to derive from the relationship linking the parameters of CJ detonation:

$$p_{CJ} = \frac{\rho_0 D^2}{k+1} \tag{14}$$

where $D$ is the detonation velocity.

In the case of the Adams and Pack model, the mass velocity $u_2$ behind the front of the combustion wave is zero. Then, from the conservation laws (9)-(11), the deflagration wave velocity as a function of parameters marked with an index 1 can be determined:

$$w^2 + \frac{w}{u_1}\left[(k-1)(q+e_1) - \frac{p_1}{\rho_1} + \frac{k-3}{2}u_1^2\right] - (k-1)\left(q + e_1 + \frac{p_1}{\rho_1} + \frac{u_1^2}{2}\right) = 0 \tag{15}.$$

After determining the value of the deflagration wave velocity from equation (15) for a given pressure $p_1$, parameters $p_2$ and $\rho_2$ can be calculated from equations (9)-(10) assuming $u_2 = 0$. In the paper [1], the following data were used for pentolite: $\rho_0 = 1.67$ g/cm$^3$, $c_0 = 2.43$ mm/μs, $q = 1160$ cal/g, $k = 2.598$. The results of calculations for the deflagration waves are presented in Table 2.

**Table 2.** The results of calculations for deflagration waves for pentolite [1] − Adams and Pack model

| $p_1$ [kbar] | $p_2$ [kbar] | $u_1$ [mm/μs] | $w$ [mm/μs] | $u_1 + c_1$ [mm/μs] |
|---|---|---|---|---|
| 1 | 0.9998 | $2.440 \cdot 10^{-2}$ | $2.489 \cdot 10^{-2}$ | 2.479 |
| 2 | 1.9984 | $4.831 \cdot 10^{-2}$ | $5.023 \cdot 10^{-2}$ | 2.527 |
| 4 | 3.988 | $9.481 \cdot 10^{-2}$ | $1.023 \cdot 10^{-1}$ | 2.620 |
| 7 | 6.937 | $1.615 \cdot 10^{-1}$ | $1.836 \cdot 10^{-1}$ | 2.753 |
| 10 | 9.815 | $2.249 \cdot 10^{-1}$ | $2.700 \cdot 10^{-1}$ | 2.880 |
| 20 | 18.75 | $4.171 \cdot 10^{-1}$ | $5.700 \cdot 10^{-1}$ | 3.264 |
| 30 | 26.36 | $5.864 \cdot 10^{-1}$ | $8.860 \cdot 10^{-1}$ | 3.603 |
| 40 | 32.56 | $7.385 \cdot 10^{-1}$ | 1.201 | 3.907 |
| 70 | 44.47 | 1.1244 | 2.054 | 4.678 |
| 100 | 50.28 | 1.4410 | 2.738 | 5.311 |
| 123.8 | 52.62 | 1.6597 | 3.186 | 5.749 |

The calculated values of the deflagration wave velocity are approximately 300 times greater than the velocity obtained from equation (3) describing the dependence of the linear burning rate on pressure. It was observed in work [17] that the deflagration wave velocities in explosives are of the order of 1-2 mm/μs, which correlates well with the results in the fourth column of Table 2. This supports the critical remarks made by the authors of [1] on Macek's extrapolation of experimental data obtained from measurements of the linear combustion velocity above the pressure of 1 kbar. Data from Table 2 also show that for pressures up to 20 kbar, the pressures $p_1$ and $p_2$ differ slightly, which means that the model of Adams and Pack in this range is similar to the model of constant pressure deflagration.

The motion trajectory of the combustion wave front can be calculated from the formula:

$$x_w(t) = \int_0^t w(\tau)\, d\tau \tag{16}$$

where $w(t)$ is determined from the dependence of $w$ on $p_2$ from Table 2, and the time-dependence of $p_2$, according to the relationship (4). Development of the combustion wave front and compression waves in pentolite on a plane $x$-$t$ are shown in Figure 5.

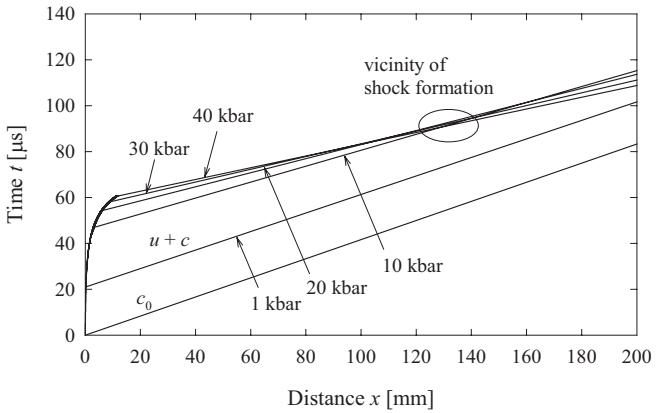


**Figure 5.** Characteristics of compression waves generated by the combustion of pentolite obtained from the Adams and Pack model.

The characteristics of $C_+$ ($u + c$) intersect in an area approximately 130 mm from the bottom of the tube after a period of approximately 90 μs after the initiation of combustion of pentolite. It is assumed that at the point of intersection of the characteristics, the shock wave is generated which is able to initiate the explosive to detonation.

The parameters of the transition of combustion into detonation estimated from the Adams and Pack model were compared with the results of calculations made on the basis of the CJ deflagration model applied to the explosive compressed by isentropic compression waves. At the flame wave front the CJ condition is fulfilled – $w = u_2 + c_2$, i.e.:

$$(w-u_2)^2 = k\frac{p_2}{\rho_2}. \tag{17}$$

Substituting relation (17) in equations (9)-(11), the following expressions for the pressure and density behind the combustion wave front are obtained:

$$p_2 = (k-1)\rho_1(q+e_1)\left[1-\sqrt{1-\frac{(2q+2e_1+p_1/\rho_1)p_1}{\rho_1(k^2-1)(q+e_1)^2}}\right] \tag{18}$$

$$\rho_2^{-1} = \frac{(k-1)(q+e_1+p_1/\rho_1)}{k\,p_1}\left[1+\sqrt{1-\frac{k^2(2q+2e_1+p_1/\rho_1)p_1}{\rho_1(k^2-1)(q+e_1+p_1/\rho_1)^2}}\right] \tag{19}$$

The deflagration velocity is then calculated from the relationship:

$$w = u_1 + \left( k \frac{p_2}{\rho_2} \right)^{1/2} \frac{\rho_2}{\rho_1} \tag{20}$$

The calculated results for pentolite are shown in Table 3 and in Figure 6. For a low initial pressure $p_1$, the pressure $p_2$ behind the CJ deflagration wave front is much lower than the pressure estimated by the Adams and Pack model, and the flame wave velocity is nearly doubled. That means that the CJ deflagration wave simultaneously moves in the explosive at a greater distance. The time of emergence of the shock wave is about 80 μs and it is slightly shorter than the time calculated for the Adams and Pack model (around 90 μs), and the distance to shock formation increases (about 140 mm in Figure 6 to about 130 mm in Figure 5). Since the applied theoretical models allow the calculation of upper and lower limits for the deflagration to detonation transition, a critical time and distance of the transition will be bracketed by these results, if the isentropic compression of pentolite can be described by the equation (2) with $n = 3$.

**Table 3.** The results of calculations for the deflagration waves for pentolite [1] – the CJ deflagration model

| $p_1$ [kbar] | $p_2$ [kbar] | $u_2$ [mm/μs] | $w$ [mm/μs] |
|---|---|---|---|
| 1 | 0.2799 | -2.044 | $4.500 \cdot 10^{-2}$ |
| 2 | 0.5637 | -2.019 | $8.910 \cdot 10^{-2}$ |
| 4 | 1.1426 | -1.958 | $1.750 \cdot 10^{-1}$ |
| 7 | 2.038 | -1.870 | $2.986 \cdot 10^{-1}$ |
| 10 | 2.966 | -1.782 | $4.170 \cdot 10^{-1}$ |
| 20 | 6.261 | -1.5253 | $7.767 \cdot 10^{-1}$ |
| 30 | 9.835 | -1.3208 | 1.096 |
| 40 | 13.65 | -1.1304 | 1.386 |
| 70 | 26.32 | $-6.539 \cdot 10^{-1}$ | 2.130 |
| 100 | 38.62 | $-2.247 \cdot 10^{-1}$ | 2.751 |
| 123.8 | 52.62 | 0 | 3.186 |

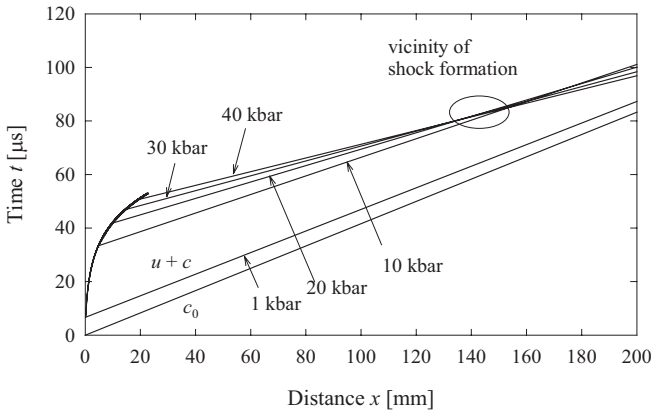


**Figure 6.** Characteristics of compression waves generated by the combustion of pentolite for the CJ deflagration model.

## Modeling of the deflagration to detonation transition in primary explosives

In the paper [1] the models described above were used to calculate the distance and time of the passage from deflagration to detonation in the primary explosive − lead azide. On the basis of experimental literature data, the time-dependence of the pressure $p_1$ for the deflagration wave in lead azide was obtained. To describe the physical properties of crystals of lead azide, the Tait equation and experimental data obtained from the relationship between pressure and mass velocity on the front of a shock wave were applied. The latter was used to calculate the mass velocity of compressed lead azide:

$$u_1 = \frac{p_1}{\rho_0 c_0} \tag{21}$$

where $\rho_0 = 4.6$ g/cm$^3$, $c_0 = 2.15$ mm/μs.

In this case, the authors of [1] did not give details of the DDT problem. Meanwhile, the use of data from the Hugoniot curve to describe the isentropic compression of the explosive is a coarse approximation. In addition, there is some ambiguity in the model associated with the calculation of the mass velocity of the compressed explosive by the use of the formula (21) and the velocity of sound, internal energy and density using the Tait model (2).

The calculated distance to the transition from deflagration to detonation in the lead azide crystal was about 2 mm, which is in good agreement with experimental data obtained for lead azide crystals of different thicknesses. In crystals with a thickness of less than 2 mm, there was no DDT phenomenon, whilst in thicker crystals this process was observed. The calculated combustion velocities for both models (Adams and Pack and CJ) are an order of magnitude smaller than the velocity of 2.7 mm/μs measured by Chaudhri and Field [18]. Despite the objections presented earlier in [1] this model was also used to calculate the process of accelerating deflagration in pressed charges of lead azide. The following data were adopted: $\rho_0 = 3.4$ g/cm$^3$, $c_0 = 1.23$ mm/μs. In this case, the distance to the creation of the shock wave was 0.9 mm. Porosity causes reduced velocity of sound in the pressed charge and hence the intersection of the relevant characteristics takes place earlier.

Due to the limited amount of experimental data for primary explosives, an attempt was undertaken to study the influence of the burning rate of these materials on the process of DDT in a typical primary explosive. In spite of previous limits, as in [1], models developed for cast explosives were used. The following parameters for the primary explosive were assumed: $\rho_0 = 1.4$ g/cm$^3$, $c_0 = 1.20$ mm/μs. The proposed value of $\rho_0$ corresponds to the density of pressed complex compounds tested in the Department of Explosives at the Military University of Technology [19], and the velocity of sound is close to the velocity in pressed lead azide [1]. The heat of combustion $q = 2000$ cal/g was derived from work [20]. It was assumed that the adiabatic exponent of the combustion products $k$ is equal to 3.2. The value of $p_0$ from equation (1) was assumed to be 0.1 kbar.

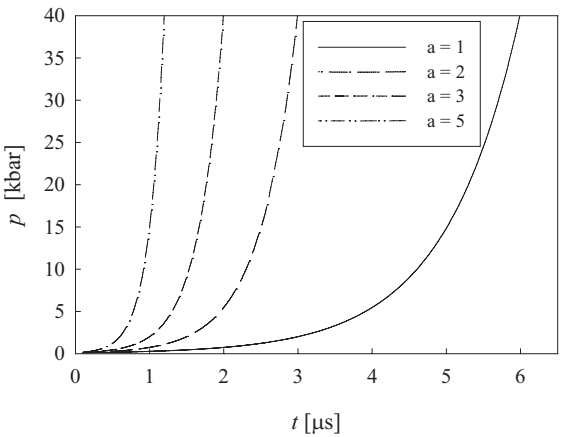


**Figure 7.** Time-dependence of pressure in the combustion products for different values of $a$ (Eq. (1)).

Initially, the influence of the burning rate of the explosive on the DDT process was investigated. The burning rate of a confined explosive is represented by the dependence of pressure on time (Eq. 1). Figure 7 shows the change in pressure for different values of $a$. The pressure builds up to a value of about 40 kbar in the period from 1 to 6 μs for changes in $a$ from 5 to 1.

To perform the calculations for a typical primary explosive the models of flame acceleration discussed in the preceding paragraph were used. Table 3 presents the parameters for the deflagration wave as a function of the pressure in the compressed explosive. The Adams and Pack and CJ models were used in the calculations. The range of changes of the pressure $p_1$ corresponds to the amplitude of shock waves leading to detonation of primary explosives (e.g. 6 kbar in the case of lead azide [21]). As previously stated, the flame front velocity $w$ and pressure $p_2$ in the combustion products behind the wave front calculated for the models from Adams and Pack and CJ are the limiting values of these parameters for the deflagration wave in the tested explosive.

**Table 3.** Results of calculations for deflagration waves in the primary explosive

| $p_1$ [kbar] | $u_1$ [mm/μs] | $u_1 + c_1$ [mm/μs] | Adams and Pack model ($u_2 = 0$) | | CJ model | |
|---|---|---|---|---|---|---|
| | | | $p_2$ [kbar] | $w$ [mm/μs] | $p_2$ [kbar] | $w$ [mm/μs] |
| 1 | $5.68 \cdot 10^{-2}$ | 1.313 | 0.9994 | $5.75 \cdot 10^{-2}$ | 0.2392 | $7.44 \cdot 10^{-2}$ |
| 3 | 0.157 | 1.514 | 2.987 | 0.162 | 0.7233 | 0.206 |
| 6 | 0.248 | 1.769 | 5.915 | 0.301 | 1.461 | 0.374 |
| 12 | 0.488 | 2.177 | 11.51 | 0.540 | 2.972 | 0.645 |
| 18 | 0.652 | 2.504 | 16.70 | 0.744 | 4.520 | 0.866 |

Figures 8-11 show the $x$-$t$ plane images of the transition from deflagration to detonation for various values of the exponent $a$ in Eq. (1). A slight difference is observed in the distances from the tube bottom to the points of creation of a shock wave for both models used. The distance of the deflagration to detonation transition in the tested porous explosive decreases from about 1 to 6 mm when the parameter $a$ is changed from 1 to 5. This change in the parameter $a$ means a significant increase in rate of pressure rise in the reaction products (Figure 7). The range of changes in distance of intersection of the characteristics obtained corresponds to the run distances to detonation in primary explosives. For example, the DDT in porous lead azide takes place over a distance of 1-3 mm depending on the duration of the loading pressure (0.1 and 3.5 μs) with an amplitude of

6-9 kbar [20]. In turn, a complex primary explosive [Cu $(C_2H_4N_4)_3$] $(ClO_4)_2$ triggers the detonation of PETN, if the length of the charge of initiating explosive is at least 4.5 mm, which means that at this distance burning must develop into detonation [19].

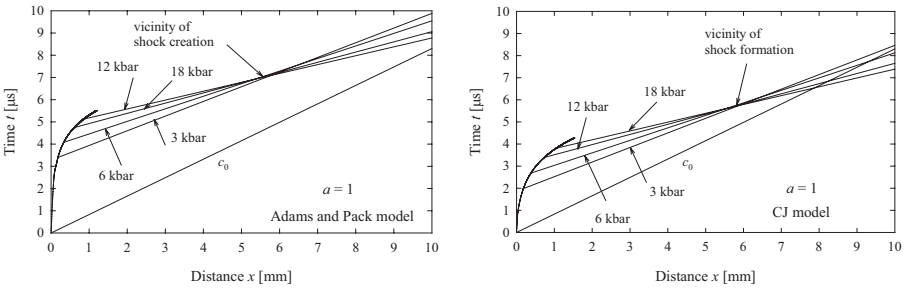


**Figure 8.** Characteristics of compression waves generated by the combustion of the primary explosive enclosed in a tube for the exponent $a = 1$.

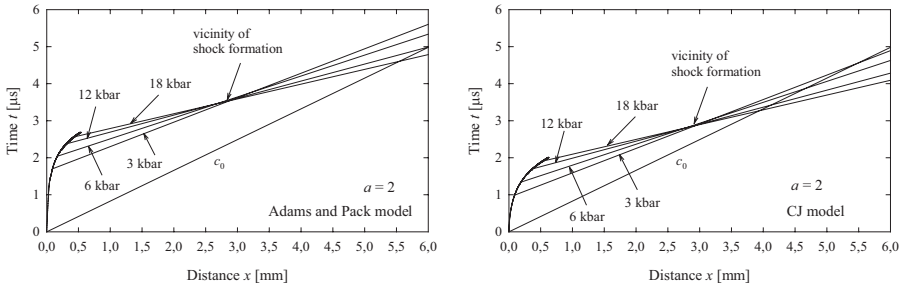


**Figure 9.** Characteristics of compression waves generated by the combustion of the primary explosive enclosed in a tube for the exponent $a = 2$.

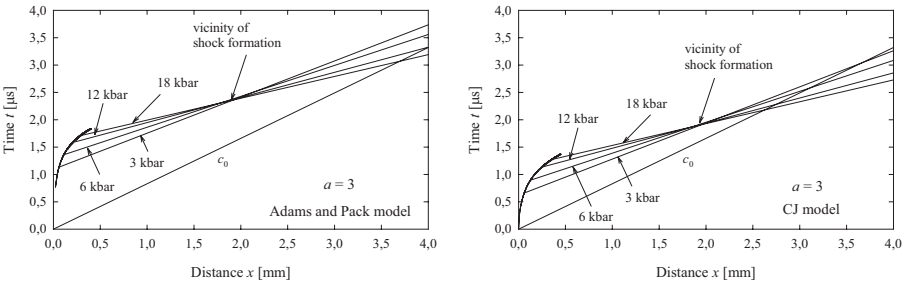


**Figure 10.** Characteristics of compression waves generated by the combustion of the primary explosive enclosed in a tube for the exponent $a = 3$.

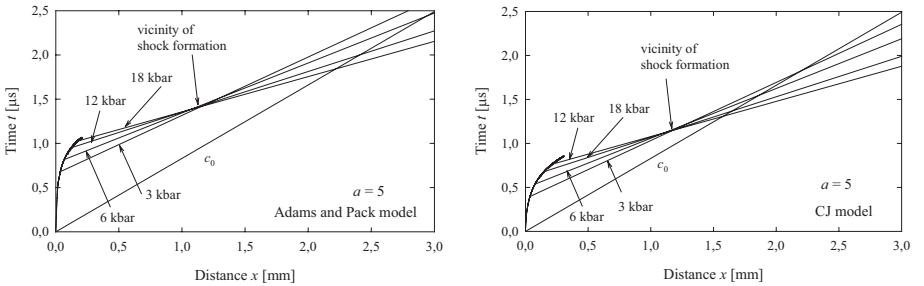


**Figure 11.** Characteristics of compression waves generated by the combustion of the primary explosive enclosed in a tube for the exponent $a = 5$.

We can compare how the deflagration front velocity evolves over time in the primary explosive for the Adams and Pack model and the CJ model. The calculated results are shown in Figure 12. In the Adams and Pack model the front velocity is lower for the same time compared with the CJ model. However, it should be noted that in the first case, the mass velocity behind the wave front is zero (Figure 4c) and the whole released reaction energy is transmitted to the explosive. Therefore, generation of a compression wave of a given pressure ahead of the front requires a lower velocity than in the CJ deflagration model, in which a part of the energy is consumed to give a negative momentum of the gaseous combustion products (Figure 4b).

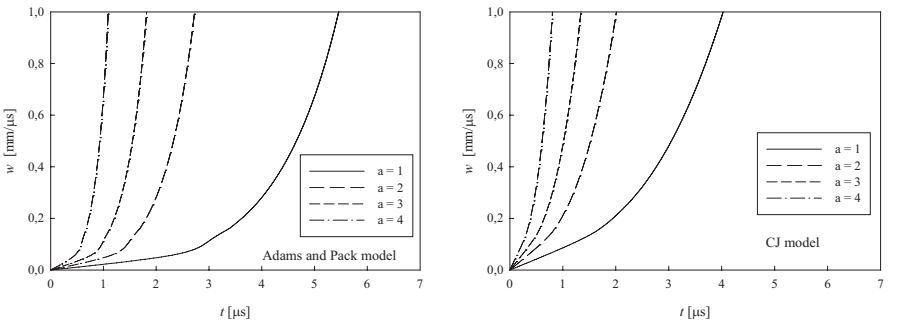


**Figure 12.** The change in time of the wave flame velocity in a primary explosive for various values of the exponent $a$.

An analysis of the position of the intersection of the characteristics in Figures 8-11 shows that the distance from the charge bottom to the intersection point is changed relatively little for a high variation in the rate of pressure rise. In order to check how the properties of the primary explosive, density and

velocity of sound, affect the location of this point, calculations for a material with a higher density were performed. For this calculation the complex material was assumed in the form of a crystal of density $\rho_0 = 2.0$ g/cm$^3$ [19] and velocity of sound $c_0 = 2.1$ mm/μs (as in crystals of lead azide). The burning parameters were identical to the parameters of the porous complex explosive tested earlier. Figure 13 shows wave images of the explosive compression by the accelerating deflagration wave for both the models used. The assumed dependence of pressure behind the front corresponds to the parameter $a = 2$ (Figure 7). A comparison of the location of points of intersection of the characteristics in Figures 9 and 13 shows that the distance to detonation in a crystalline material with a high density is more than twice that in the case of a porous material.

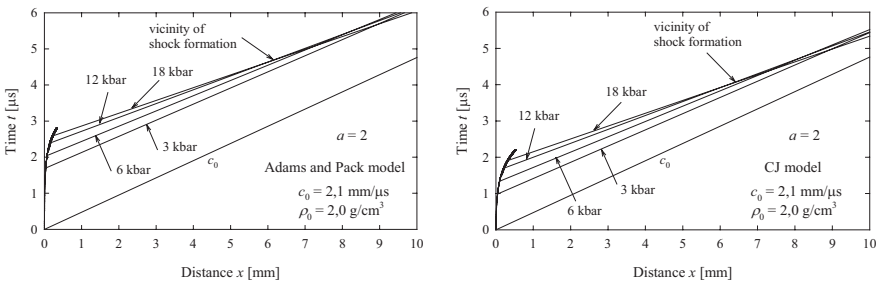


**Figure 13.** Characteristics of compression waves generated by the combustion of the primary explosive of high density.

## Summary

The application of the model of accelerating deflagration in cast explosives to a description of the transition from combustion to detonation in primary explosives allowed us to obtain results consistent with experimental data in quantitative terms. Thus, the estimation of the velocity of a flame wave front which leads to initiation of a primary explosive to detonation is possible. However, a more accurate assessment of the front velocity and the passage from burning to detonation will be achievable only on the basis of experimental measurements of the time-dependence of the pressure in reaction products behind the deflagration wave front. In the case of porous explosives more precise prediction of the DDT parameters requires the use of complex theoretical models, which better describe the phenomena of accelerating deflagration in these materials. This in turn leads to the need to solve the DDT problem by application of the numerical methods used in fluid dynamics, for example, the method of differential schemes.

## References


[1] Tarver C.M., Goodale T.C., Shaw R., Cowperthwaite M., Deflagration-to-Detonation Transition Studies for Two Potential Isomeric Cast Primary Explosives, *Sixth Symposium (International) on Detonation*, Office of Naval Research, White Oak, **1976**, p. 231.

[2] Macek A., Transition from Deflagration to Detonation in Cast Explosives, *J. Chem. Phys.,* **1959**, *11*(1), 162-167.

[3] McAfee J.M., Asay B.W., Campell A.W., Ramsay J.B., Deflagration to Detonation in Granular HMX, *Ninth Symposium (International) on Detonation*, Office of Naval Research, Portland, **1989**, p. 265.

[4] McAfee J.M., Asay B.W., Bdzil J.B., Deflagration-to-Detonation in Granular HMX: Ignition, Kinetics, and Shock Formation, *Tenth International Detonation Symposium*, Office of Naval Research, Boston, **1993**, p. 716.

[5] Parker G.R., Dickson P., Asay B.W., McAfee J.M., DDT of Hot, Thermally Damaged PBX 9501 in Heavy Confinement, *Fourteenth International Detonation Symposium*, Coeur d'Alene Resort, **2010**, ID 41284.

[6] Gifford M.J., Proud W.G., Field J.E., *Observation of type II deflagration-to-detonation transitions*, CP620, Shock of Condensed Matter –2001, American Institute of Physics, **2002**.

[7] Field J.E., Walley S.M., Pround W.G., Balzer J.E., Gifford M.J., Grantham S.G., Greenaway M.W., Siviour C.R., The Shock Initiation and High Strain Rate Mechanical Charcterization of Ultrafine Energetic Powders and Compositions, *Mat. Res. Soc. Symp. Proc., vol. 800*, AA5.4.1, Materials Research Society, **2004**.

[8] Walley S.M., Field J.E., Greenaway M.W., Crystal Sensitivieties of Energetic Materials, *Materials Science and Technology*, **2006**, *22*(4), 402.

[9] Pround W.G., Walley S.M., Willianson D.M., Collins A.L., Addiss J.W., Recent Trends in Research on Energetic Materials in Cambridge, *Cent. Eur. J. Energ. Mater*., **2009**, *6*(1), 67-102.

[10] Bdzil J.B., Menikoff R., Son S.F., Kapila A.K., Steward D.S., Two-phase Modeling of Deflagration-to-Detonation Transition in Granual Materials: A Critical Examination Of Modeling Issues, *Physics of Fluids*, **1999**, *11*(2), 378-402.

[11] Kapila A.K., Menik**off** R., Bdzil J.B. Son S.F., Steward D.S., Two-phase Modeling of Deflagration-to-Detonation Transition in Granual Materials: Reduced equations, *Physics of Fluids*, **2001**, *13*(10), 3002-3024.

[12] Narin B., Ozyoruk Y., Ulas A., Application of Parallel Processing to Numerial Modeling of Two-phase Deflagration-to-Detonation (DDT) Transition Phenomenon, in: *Parallel Computation Fluid Dynamics* (I.H. Tuncer et al.) **2007**; DOI: 10.1007/978-3-540-92744-0_15, Springer-Verlag Berlin Heidelberg **2009**.

[13] Fogelzang A.E., Sinditski V.P., Egorshev V.Y., Serushkin V.V., Effect of Structure of Energetic Materials on Burning Rate, *Proceedings of Symposium on Decomposition, Combustion, and Detonation Chemistry of Energetic Materials*, Boston, **1995**, Materials Research Society, *vol. 418*, p. 151.

[14] Adams G.K., Pack D.C, Some Observations on The Problem of Transition Between Deflagration and Detonation, *Seventh Symposium (International) on Combustion*, Butterworths, London, **1959**, p. 812.
[15] Troshin Ya.K., The Generalized Hugoniot Adiabatic Curve, *Seventh Symposium (International) on Combustion*, Butterworths, London, **1959**, p. 789.
[16] Price D., Wehner J.F., ThE Transition From Burning to Detonation in Cast Explosives, *Combustion and Flame*, **1972**, *9*, 419.
[17] Gibson R.W., Macek A., Flame Fronts and Compression Waves During Transition from Deflagration to Detonation In Solids, *Eighth Symposium (International) on Combustion*, Williams and Wilkins, Baltimore, **1962**, p. 847.
[18] Chaudhri M.M., Field J.E., Deflagration in Single Crystals of Lead Azide, *Fifth Symposium (International) on Detonation*, Office of Naval Research, Pasadena, **1970**, p. 301.
[19] Cudziło S., *Complex compounds with explosive properties*, Private Communication, **2009**.
[20] Fridrich M., Gilvez-Ruiz J.C., Klapotke T.M., Mayer, P. Weber B., Weigand J.J., BTA Copper Complexes, *Inorganic Chemistry*, **2005**, *44*, 8044-8052.
[21] Davies F.W., Zimmerschied A.B., Borgardt F.G., Avrami L., The Hugoniot and Shock Initiation Threshold of Lead Azide, *Sixth Symposium (International) on Detonation*, Office of Naval Research, White Oak, **1976**, p. 389.